P3.4 POSSIBLE IMPROVEMENTS IN THE STANDARD ALGORITHMS FOR TRMM/PR

Nobuhiro Takahashi* and Toshio Iguchi

National Institute of Information and Communications Technology

1. INTRODUCTION

The latest version (version 6) of the TRMM rain products (PR and TMI) seem to be closer each other within 10-15% difference based on zonal mean monthly data. However, both products still show inconsistency each other, for example, simultaneous estimations show scattered pattern even for the stratiform rainfall over ocean (Takahashi, 2006). In addition, a recent report that compares rainfall amount between a rain gauge network and PR over China shows about 30 % underestimation of PR during warm seasons (Yatagai and Xie, 2006). This result indicates that the PR algorithm still have room for improvements. One possible way to improve the current standard algorithm for TRMM/PR (level 1 and 2 algorithms) is to re-examine assumptions and models used in PR algorithms which are compliment information that cannot be obtained or determined by the radar observation. For example, vertical profile of hydrometeor type cannot be determined by only the reflectivity information of single frequency radar except for the special case such that bright band appears in the stratiform rain.

The purpose of this study is to evaluate the assumptions and physical models used in the PR algorithms. One of the approaches of this study is to utilize long term (trend) data in order to obtain the information that cannot be obtained or determined by simultaneous observation. Another approach is to evaluate the algorithm by comparing with the measurements other than TRMM/PR such as ground based observation.

2. STANDARD ALGORITHMS FOR TRMM/PR

The structure of the TRMM/PR standard algorithm is overviewed in this section and the improvement items are identified from assumptions and models introduced in each algorithm. Figure 1 describes the structure of level 1 and 2 algorithms for TRMM/PR with their products

The level 1 algorithm produces not only the observed radar reflectivity factor but also system noise level, rain/no-rain classification, surface echo peak range bin, echo top height, and so on. Among them, rain/no-rain classification algorithm may have an impact to the rain estimation except for the radar reflectivity factor itself which depends on the calibration of the radar (but we don't discuss on the calibration issue in this paper). The peak surface echo is used for estimation of the path integrated attenuation (PIA) in 2A21 which major products are the power of the Earth surface echo and PIA. Since the peak surface echo range bin is determined by 1B21, PIA estimation in 2A21 along with surface echo profile and its peak range bin in 1B21 is also considered in this study.

The 2A23 algorithm owes the rain type (i.e. convective or stratiform) classification that depends mainly on the detection of the bright band (BB). The miss-classification of rain type leads to use the inappropriate Z-R model. The rain retrieval algorithm introduces different Z-R relationship for convective and stratiform rainfall, respectively. Since the input to this algorithm is level 1 product which is affected by the attenuation, there is chance to miss-judge BB in this algorithm.

The 2A25 algorithm is the main body for the rain estimation. Therefore, a lot of parts that directly influence the rain estimation are included in this algorithm. The DSD model (Z-R relationship) directly affect the rain estimation and the correction of non-uniform beam filling (NUBF) effect contains large uncertainty, as well as the assumptions of the vertical profile of hydrometeor type. In this study, we try to evaluate DSD parameter estimated by 2A25 algorithm. Also we focus on the NUBF effect to the PIA estimation.

3. EVALUATION OF THE ALGORITHM

In this section detailed evaluation and improvement are explained for each items listed in the previous section.

3.1 EVALUATION OF RAIN/NO-RAIN CLASSIFICATION ALGORITHM IN 1B21

The rain/no-rain classification algorithm in 1B21 can be improved especially over ocean. The problem of the current product is that the "rain possible" pixels cannot be used for level 2 processing because of the contamination of the noise pixels among rain pixels (probably contamination of rain pixels among noise pixels, that is, too many false "rain possible" pixels). For better classification of the "rain possible", the system noise data that is used as the reference for the rain/no-rain classification algorithm must be evaluated first. In 1B21, the "rain possible" and "rain certain" pixels are identified if the observed data (except for ground clutter) exceed the threshold value of the observed instantaneous system noise level (Kumagai et al., 1996) for continuous three range bins (750 m in range). Therefore the characteristics of the system noise is analyzed.

The major sources of the fluctuation of the system noise are fading effect (number of samples for system noise of each angle bin is 256 for PR), changes in the

*Corresponding author address: Nobuhiro Takahashi, National Institute of Information and Communications Technology (NICT), 4-2-1 Nukuikita-machi, Koganei-shi, Tokyo 184-8795 JAPAN; email: ntaka@nict.go.jp

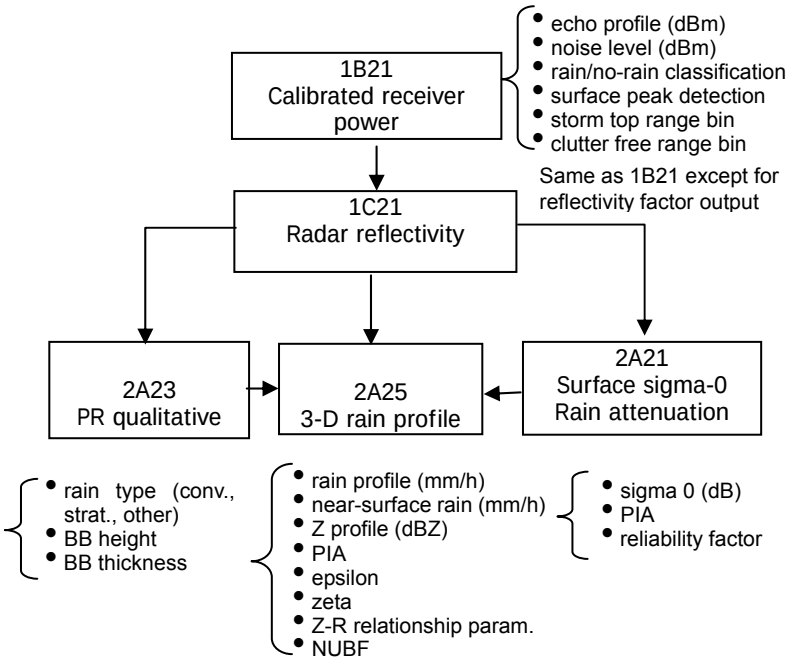

Fig.1. Structure of level 1 and 2 algorithm for TRMM/PR (modified from TRMM/PR algorithm instruction manual, TRMM precipitation radar team, 2005)

temperature at the radar receiver, degradation of the receiver system and the emission from the Earth. For this reason that current algorithm considers all of these items including the drift of the system noise level with time. The contribution of each item is obtained by using long term data; the fading effect is evaluated by the histogram of the observed data under a stable Earth surface condition. The fluctuation of receiver temperature is obtained to see the averaged system noise over one orbit over ocean to remove the fading effect and its long term trend clarifies the long term receiver performance. The residual is the emission from the Earth. Takahashi and Iguchi(2004) has already analyzed long term trend of the system noise and shows that PS's system noise is very stable with time and the major fluctuation source of the system noise is the fading effect.

Based on this result a new over ocean rain/no-rain classification algorithm is developed with a fixed threshold in 1B21 algorithm and processing of higher level standard algorithm is conducted from the 1B21 product with new rain/no-rain classification. The reference noise level is determined from the statistics of the system noise under no-rain condition. The selected thresholds are 99% and 99.99% levels of the accumulated probability. In the new product, "rain possible" pixels decreases significantly and they are confined around the "rain certain" pixels (see Fig. 2, an example of new classification). Therefore the new "rain possible" pixels can be regarded as rain pixels. The new rain/no-rain classification algorithm increases

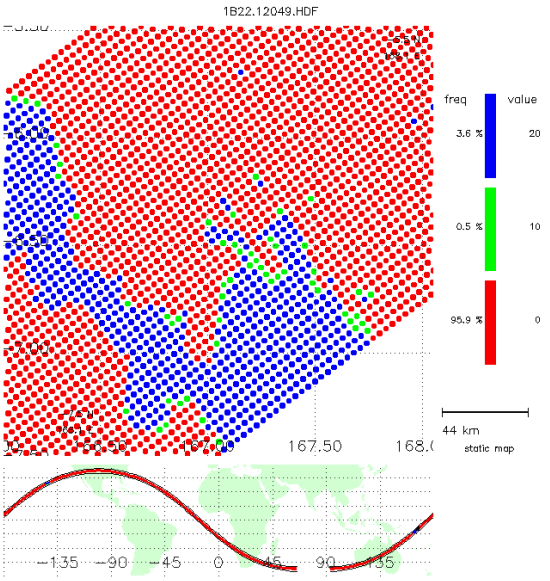

Fig.2. Example of new rain/no-rain classification proposed in this study. This figure is taken from the TSDIS orbit viewer. The area with the value of 20 is "rain certain" and 10 is "rain possible"

the rain area by more than 10% from the "rain certain" area of current 1B21 and increases the rainfall amount by about 1% when the new "rain possible" pixels are included.

3.2 PIA ESTIMATION ALGORITHM IN 2A21

One of the issues on the PIA estimation algorithm (2A21) is the uncertainty of PIA relating to the NUBF effect. This data is closely related to the level 1 algorithm that determines the surface peak location. Under the non-uniform beam filling condition the surface echo peak location (range bin) shifts from the actual surface location (range bin) (Takahashi et al., 2006) and it leads erroneous PIA estimation. If the algorithm uses reliable topography data, this problem can be reduced to some extent (actually current level 1 algorithm does not use a reliable elevation map). Precise elevation map is not enough considering the radar beam width and the observation with various incident angles at complex terrain. One possible way to overcome this issue is to create reference data with high special resolution obtained under no-rain condition. It should be noted that this issue is common with the expected algorithm for dual frequency precipitation radar onboard the Global Precipitation Measurement (GPM) core satellite. Figure 3 shows an example how the NUBF effect changes the PIA estimation. This profile is observed over Bolivia as a part of convective system. The topography of this area is flat. In this figure, both the Z profiles of 1C21 and 2A25 are shown in order to evaluate how the attenuation recovered by 2A25 from 1C21. This figure also compares the surface echo profile with no-rain surface echo profile sampled very close to the observation point (distance is 1.3 km and the data is not sampled on the same day). The peak range bin location of surface echo offsets several range bins from the peak of the reference profile and the surface echo profile is very thin comparing with the reference profile indicating the non-uniform rainfall. If the surface peak power compared with the reference peak power (this is the way of 2A21), the PIA is about 10 dB (actually, the PIA in 2A21 is about 10 dB). On the other hand the estimated PIA will reach 30 dB if the same range bin data are compared.

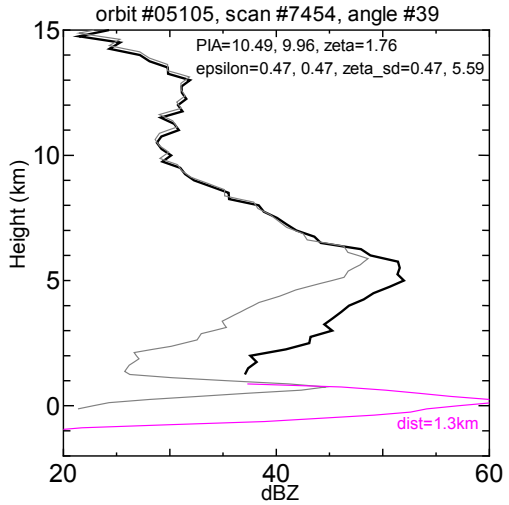

Fig.3. Example of vertical profile reflectivity factor from 1C21 and 2A25 affected by the non-uniform beam filling effect.

In this study, high spatial resolution surface peak echo data set (range bin number relative to the Earth ellipsoid and its echo power) under no-rain condition is created to evaluate the surface peak detection globally and the estimation error of PIA in 2A21 algorithm. To establish the high spatial resolution data (e.g. 0.01 or 0.02 degree in latitude and longitude for each incident angle), several years of data is needed to fill all grids. The problem of this approach is that the surface peak echo power changes with the surface condition (such as wind speed over ocean and seasonal change of vegetation over land). For this reason, surface peak location (range bin relative to the Earth ellipsoid) map is created to obtain the appropriate surface peak position. The dataset is expected to be quite similar to the topography map, especially over ocean. Only slight differences among different incident angles appear almost all global area except for mountainous region such as Himalayan mountains, Tibetan plateau and Andes mountains.

The differences in range between peak surface echo bin (binSurfPeak in 1B21) and range bin of the Earth ellipsoid from the satellite (binEllipsoid) are plotted against the rain rate (2A25 near-surface rain). Figure 4 shows the result of angle bin 1 (scan angle is about 17 degrees from nadir) over ocean. Considering that binSurfPeak and binEllipsoid should appear almost the same range bin over ocean, the NUBF effect appears as the shift of surface peak position, and non-uniformity is larger in the heavy rainfall condition, the difference between binSurfPeak and binEllipsoid increases with the rain rate as shown in the figure. Since the 2A21 calculate difference in

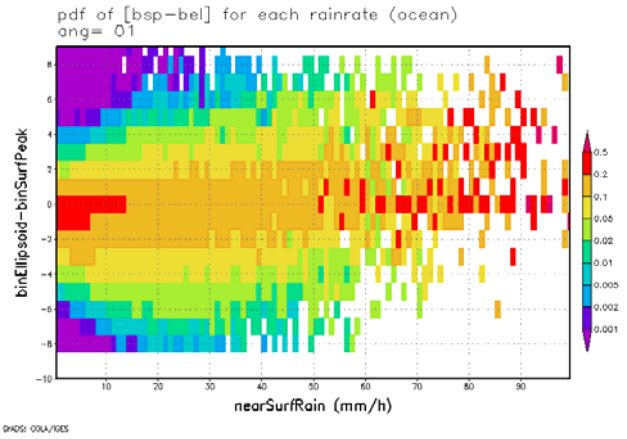

Fig.4. Probability of difference in the binSurfPeak and binEllipsoid against the rain rate obtained by 2A25 for the case of angle bin 1 over ocean.

the peak echo power between the no-rain condition and rainy condition for PIA assuming uniform rainfall, the obtained PIA may be underestimated by the NUBF effect.

Underestimation of PIA is calculated assuming the Gaussian shape surface echo profile (which is quite close to the no-rain surface echo) for each angle bin (Fig. 5 for the angle bin 1). For wider scan angle (angle bin 1), large underestimation greater than 3 dB appears even the rain rate is less than 5 mm/h. The fraction of such a large value is less than 5 % if the rain rate is less than 5 mm/h and increases up to about 20 % as the rain rate increases. Rough estimation of the increase of rainfall amount is more than 10 % for the rain rate greater than 10 mm/h (surface reference technique with PIA information works about this rain rate). Since the occurrence of heavy rain rate (e.g. 10 mm/h) is less than 5 %. Therefore the overall increase by rainfall amount may be small. In addition, the effect of the surface peak detection error becomes smaller as the scan angle approaches to the nadir. However, the underestimation of heavy rainfall may be serious for the rain system over land. Long term processing of standard algorithm is planned with the newly estimated PIA in order to assess the impact of the current 2A21 algorithm.

For the land case, detailed terrain model (surface echo profile data set) is needed to evaluate the underestimation of PIA because of complex topography comparing with ocean. A database with 0.01 degree in latitude and longitude, 49 incident angles, ascending/descending node and 10 range bins around the surface peak is desired if we estimate the NUBF effect from the profile data. Figure 6 shows an example of surface echo profile together with the no-rain profiles of different distance from the target echo. The observed surface echo is quite different from the Gaussian shape even relatively light rain condition, indicating that complex terrain. The no-rain profile close to the target pixels (0.5 km in distance) shows similar to the observed profile. As the distance increased the profile shape becomes different from the observation profile that leas erroneous calculation of PIA. This result indicates that required grid spacing of the database is al least less than 3 km. Planned database has grid spacing of 0.01 degrees.

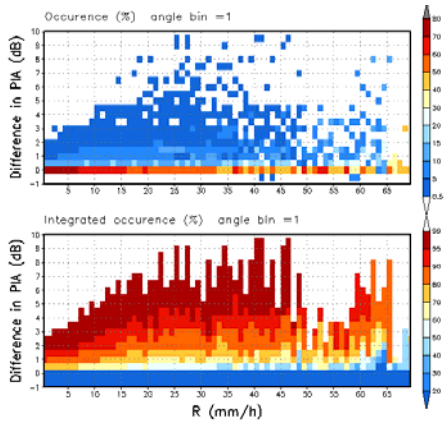

Fig.5. Probability (top) and accumulated probability (bottom) of underestimation of PIA against the rain rate for the case of angle bin 1. Difference in PIA is estimated by assuming the Gaussian shape profile

3.3 BRIGHT BAND MODEL IN 2A23 AND 2A25

Another issue in the level 2 algorithm is the bright band detection algorithm (2A23, it is rain type classification algorithm and the bright band is an indicator of stratiform rainfall); current version uses reflectivity profile data in level 1 product, which is not corrected the rain attenuation, to detect the bright band (see Fig. 1). Therefore the there are high possibility to miss-classify the rain type especially for the heavier rainfall cases because the significant attenuation begins at the top of the liquid phase (rain top, not echo top) and the attenuation is accumulated toward the surface results in an echo peak near the freezing level. So the current bright band detection algorithm should be evaluated by using such as an un-attenuated ground based radar observation and/or the attenuation corrected profile data such 2A25 product.

The characteristics of a rain system observed on June 2, 2006 (orbit #37315) is compared with ground based C-band polarimetric radar (COBRA owned by NICT, Nakagawa et al., 2003). Pixels of PR with the near-surface rain rate greater than 10 mm/h is selected and compared with the ground based

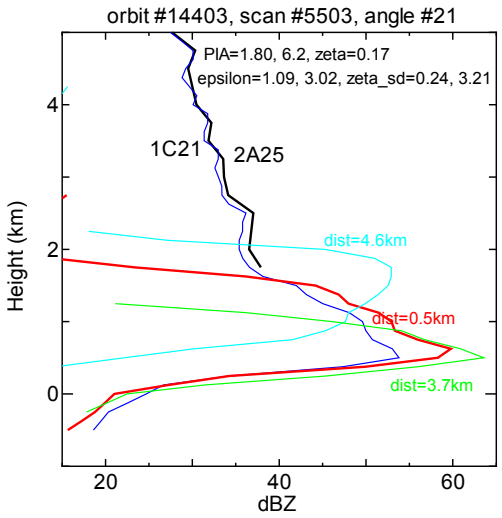

Fig.6. Example of vertical profile of surface echo over land with reference no-rain profile adjacent of the target pixel. The distance of the reference profile is 0.5, 3.7 and 4.6 km.

observation. Six pixels are identified as stratiform by 2A23 among 18 pixels that have rain rate (of 2A25) greater than 10 mm/h. Vertical structure of the stratiform echo identified by the PR is examined by COBRA data. Clear bright band cannot be seen in the COBRA data indicating miss-judgment of bright band with the level-1 data. Comparison of the vertical profiles of Z from 1C21 and 2A25 indicates that the BB-like structure seen in 1C21 profile disappeared after the attenuation corrected profile in 2A25. In addition, vertical profile of polarimetric parameters (ZDR and phv) of COBRA both of convective rain and stratiform rain (again, stratiform rain is determined by 2A23 and rain rate is greater than 10 mm/h) shows quite similar pattern each other. This result also support that 2A23 algorithm miss-judges bright band in this case. Therefore, it is worth to implemented the convective/stratiform classification algorithm (2A23) with the attenuation corrected data. One possible way is to put the 2A23 algorithm after the 2A25 calculation. Since 2A25 needs the rain type information, 2A25 first run with fixed rain type, after the 2A23 processing it runs gain with the 2A23 rain type information

Relating to the bright band, the bright band model used in the PR's algorithm (2A25) must be evaluated, that is, the attenuation properties of the bright band should be evaluated. It is because the attenuation is important for the rain retrieval algorithm and attenuation mainly occurs in the liquid precipitation and mixed phase (melting ice and snow) precipitation (i.e. bright band). It may cause the error source in the retrieved rain rate if the current model has biased attenuation information.

The attenuation property of the bright band is evaluated to see the relationship between the PIA and the rain rate for fixed freezing height over ocean (freezing height is determined by the bright band height and the freezing height model used in the PR

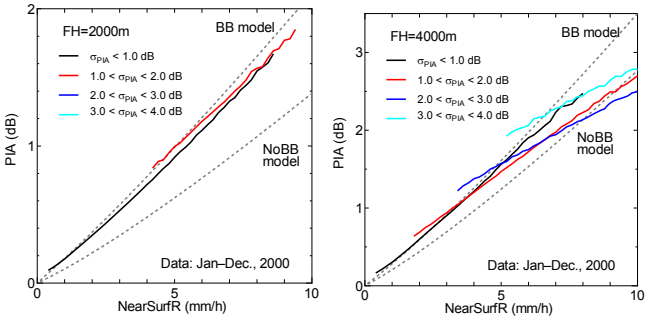

Fig.7. The relationship between near-surface rainfall and PIA for the freezing height of 2 km and 4 km with various uniformity parameter (standard deviation of PIA within TMI 10 GHz footprint size, σ_{PIA}). Dashed lines express the model calculation with bright band model (BB model) and without bright band model (NoBB model).

algorithm should also be improved). If we fix the depth of liquid and mixed-phase precipitation for given rain rate, we can deduce the attenuation from the bright band. In particular, shallower liquid precipitation layer gives more reliable information of melting layer. In this analysis we assume the horizontally and vertically uniform rain (e.g. TMI's footprint size, 60x40km of area) to compare with the 1-dimensional model. This assumption is plausible because the bright band appear in the stratiform rainfall. Since the observed PIA fluctuates by fading effect, incident angle, sea surface condition, and the non-uniform beam filling effect, long term data is needed to extract the relationship between PIA and rain rate (NUBF effect on the PIA estimation may be negligible for stratiform rainfall).

Figure 7 shows the result of the relationship between near-surface rain rate and PIA from observation and model for the freezing height of 2km and 4km and for various non-uniform condition (non-uniformity is expressed by the standard deviation of PIA with the given area= σ_{PIA} in Fig. 7) along with the model calculation based on the bright band model by Nishitsuji et al. (1983). For the widely uniform case (low σ_{PIA}) the observed relationship between rain rate and PIA is close to the model result up to 8 mm/h for the case of freezing height of 2km. As the non-uniformity increases the PIA become smaller approaching to the no-BB model. This result indicates the BB model used in 2A23 is relatively reliable in terms of attenuation in the BB.

3.4 DSD MODEL IN 2A25

The DSD model is one of the big issues for rain retrievals of spaceborne sensors (not only PR but also microwave radiometers). Current 2A25 algorithm

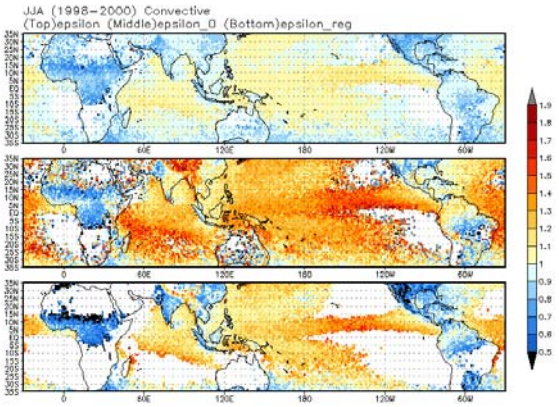

Fig.8. Three year statistics of epsilon of JJA (June, July and August) by three different methods epsilon from 2A25 (top), epsilon0 from 2A25 (middle) and epsilon of regression method (bottom).

has two major types of DSD model (Z-R relationship): one is for convective and the other is for stratiform rainfall) and the 2A25 algorithm produces one-parameter DSD information (it is called epsilon, Iguchi et al., 2000) which modifies the default Z-R relationship as the DSD parameter in 2A25 if the PIA data is applicable. The appropriate default DSD parameter can be obtained from the statistics of the epsilon. If the resultant epsilon is not unity, the default DSD (Z-R) model should be changed. Since 2A25 calculates epsilon with a statistical approach only when the PIA data is reliable (otherwise epsilon is unity) (Iguchi et al., 2000), the resultant statistics of epsilon is biased. Another output DSD parameter from 2A25 is epsilon0 which calculate the epsilon only PIA is reliable and fully trusts the PIA information (it neglects the fading effect and so on). Therefore the statistic of epilon0 has some bias.

In this study, a new epsilon is estimated by using all observation data and independent from retrieval algorithm, that is, epsilon is directly estimated from observed values (PIA and zeta) to avoid the biased epsilon information. The value zeta is defined as, $0.2\ln 10\int \alpha Z_m^{\beta} ds$ (integrated from rain top to the bottom), where α and β are coefficients in k-Z relationship, $k = \alpha Z^{\beta}$, and Z_m is observed reflectivity factor. Since the PIA fluctuates as mentioned in section 2.2, larger number of data is needed to reduce the fluctuation effect and to cover the wide range of data (both PIA and zeta). The relationship between zeta and $(1-10^{\beta \cdot PIA/10})$, has linear relationship if there is a dominant epsilon, so a linear regression is performed for each season using three years of data. A detailed DSD parameter (epsilon) map (1 x 1 degree box, separately processed for the convective and stratiform rainfall) is created for three different methods shown in Fig. 8. It is common among three estimates that the clear contrast is shown between land and ocean indicating the necessity of DSD model for land and ocean separately. In addition, estimated epsilon differs location by location. These facts indicate that the default DSD model should be allocated small area (probably) and season. Comparing with the global map of the average epsilon obtained from 3A25 product, the epsilon map in this study shows quite similar pattern with the 3A25 but larger amplitude. Estimated epsilon by the regression method correlate well with the epsilon of 2A25 but the amplitude (range of epsilon) is twice large as 2A25. This is mainly because the epsilon is determined as unity if the PIA information is not reliable in 2A25. The map of epsilon0 shows larger amplitude than other two estimates. This is caused by the epsilon0 tend to choose the high PIA cases for the epsilon calculation.

5. DISCUSSION AND SUMMARY

In this study several parts of the rain retrieval algorithm for TRMM/PR are identified to be improved. These improvements are planned to be added to the standard rain retrieval algorithm for PR and tested. Issues in the improvements are discussed in this section.

On rain/no-rain classification algorithm, it is required to develop better classification to save the rain pixels in the “rain possible” categories over land. Since the surface emission and its fluctuation is larger over land than that over ocean, it is difficult to improve the current algorithm. The approach similar to this study is worth to try, but the statistic of system noise should be developed in terms of location and season to consider the locality.

The issue to utilize the high resolution surface echo profile for the improvement of PIA estimation is that the size of data base is too huge to handle. Simpler method is needed. Though current 2A21 algorithm calculate the PIA by using peak surface echo, NUBF effect appears in the surface echo profile data should be reflected in the rain retrieval. It may be useful to deuce the NUBF and retrieve average rain within a footprint without using statistical relationship of NUBF parameter which is installed 2A25 algorithm. The issue of this method is that this method is applicable only off nadir angles (e.g. > 5 degree scan angle).

Current plan on improvement of rain type classification is as follows: 2A25 algorithm with fixed rain type (e.g. convective) implemented before 2A23 implementation in order to create attenuation corrected profile, then 2A23 is implemented for rain type and finally 2A25 is implemented again with the rain type information. The idea behind this procedure is to minimize the modification of current standard algorithm to realize better rain type classification. The impact of the miss-judge of rain type on the rain estimation is expected to be clarified quantitatively and the result of the new products should be evaluated with the ground based observation. One possible issue of this improvement is that the processing time caused by the twice implementation of 2A25.

One of the issues on the DSD model is that the relationship between PIA and zeta may not be expressed by single parameter, epsilon. That means the relationship between zeta and $1-10^{\beta \cdot PIA/10}$ cannot be expressed by a linear line. Therefore more appropriate expression is needed to express the DSD parameter. For more accurate rainfall estimation, global map of epsilon shown in Fig. 8 should be applied to determine the default Z-R relationship. However, this approach has high dependency on the climatological epsilon value such as shown in Fig. 8. The impact of the default DSD parameter should be evaluated quantitatively.

Other than these improvements shown in this study, several important improvements are remained; the most important theme is the precipitation model above freezing level. Current algorithm uses simple model that has linear change in k-Z relationship from 1 km above the freezing level to the echo top for convective rain. That means the rain-snow mixture exists to the

echo top. The precipitation type such as snow, graupel and hail should be model properly. Though it may be difficult to distinguish by single frequency reflectivity data, external information such as LIS may be helpful. Relating to this issue, rain/snow classification at the ground level is not considered in the current algorithm. It will be important to consider the water circulation and important for the high latitude precipitation measurement in GPM era.

ACKNOWKEGEMENTS

This work is conducted as a part of the Global Satellite Mapping of Precipitation (GSMaP) project supported by the Core Research for Evolutional Science and Technology (CREST) program of Japan Science and Technology Agency (JST). Some of the figures are drawn by GrADS software.

REFERENCES

Iguchi, T., T. Kozu, R. Meneghini, J. Awaka, and K. Okamoto, 2000: Rain-profiling algorithm for the TRMM precipitation radar, J. Appl. Meteor. , vol. 39, pp. 2038-2052.

Kumagai, H., T. Kozu, and T. Iguchi, 1996: Development of an algorithm for rain/no-rain discrimination, Review of the Communications Research Laboratory, Vol. 42, No. 3, pp. 317-323.(in Japanese)

Nakagawa, K., H. Hanado, S. Satoh, N. Takahashi, T. Iguchi, and K. Fukutani, 2003: Development of a new C-band bistatic polarimetric radar and observation of typhoon events. Proc. 31st Conf. on Radar Meteor., Seattle, Amer. Meteor. Soc., 863–866.

Nishitsuji, A., M. Hoshiyama, J. Awaka, and Y. Furuhama, 1983: An analysis of propagative character at 34.5 GHz and 11.5 GHz between ETS-II satellite and Kasima station. - On the precipitation model from stratus, IEICE Trans. (Japanese Edition), Vol. J66-B, 1163-1170. (in Japanese)

Takahashi, N., H. Hanado and T. Iguchi, 2006: Estimation of path-integrated attenuation and its non-uniformity from TRMM/PR range profile data, IEEE Trans., Geo. and Remote Sense., 44, 3276-3283.

Takahashi, N., and T. Iguchi, 2004: The characteristics of system noise of TRMM/PR and their application to the rain detection algorithm, IGARSS 2004, Anchorage.

Takahashi, N., 2006: Comparison of instantaneous rain rate of stratiform rainfall from TRMM/TMI with PR, IGARSS 2006, Denver.

TRMM Precipitation Radar Team, 2005: Tropical Rainfall Measuring Mission (TRMM) Precipitation Radar algorithm Instruction manual for version 6, JAXA and NASA, 175 pp.

Yatagai, A. and P. Xie, 2006: Utilization of a rain-gauge-based daily precipitation dataset over Asia for validation of precipitation derived from TRMM/PR and JRA-25, SPIE 2006, 6404-53.